Assessments of Recent GRACE and GOCE Release 5 Global Geopotential Models in Canada

Jianliang Huang and Marc Véronneau
Canadian Geodetic Survey, SGB, Natural Resources Canada
588 Booth Street, Ottawa, Ontario, Canada, K1A 0Y7
E-mails: Jianliang.Huang@NRCan-RNCan.gc.ca; Marc.Veronneau@NRCan-RNCan.gc.ca

Abstract

The objective of this study is to assess the recent GRACE and GOCE release 5 (R5) global geopotential models (GGM) in Canada. For the evaluation of the GGM against GPS-Levelling data and deflections of the vertical, the satellite models need to be combined with terrestrial gravity data to determine high-resolution geoid models. This process allows a significant reduction of the omission error in the satellite gravity models. The geoid computation is founded on the remove-compute-restore Stokes-Helmert scheme, in which the Stokes kernel function modification is used to constrain the regional geoid models to the spectral bands of the satellite model to be assessed. The resulting geoid models are directly comparable to the GPS-Levelling data, and these same geoid models can be used to derive deflections of the vertical which are compared to astronomic deflections. The data analysis indicates that the GOCE R5 models provide better precision than the GOCE release 4 (R4) models beyond degree and order 180. The accuracy of the GOCE R5 models is estimated to be better than 4-5 cm up to spherical harmonic degree ~200. The astronomic deflections appear not accurate enough to measure improvements in the GOCE R5 models with respect to the GOCE R4 models. For the validation of GGM against terrestrial gravity data over land, EIGEN-6C4, which includes a GOCE R5 model, is assessed in contrast to EGM2008. Our analysis infers that the GOCE contribution in EIGEN-6C4 is more accurate than the corresponding wavelength components in EGM2008, which includes the Canadian terrestrial gravity data.

1 Introduction

The Gravity field and steady-state Ocean Circulation Explorer (GOCE) satellite by European Space Agency (ESA) was launched on March 17th, 2009, and re-entered the Earth's atmosphere falling into the ocean on November 11th, 2013. Its objectives were to measure the Earth's gravity field with an accuracy of 1 mGal (one millionth of the Earth's gravity) and geoid with an accuracy of 1-2 cm at a spatial resolution of 100 km. Since the first release of GOCE models in 2010, four more generations of GOCE-only and GOCE-based satellite global geopotential models (GGM) have been made available publically. This paper will look into the latest two releases. Simultaneously, geodesists resumed the development of GGM from the ongoing twin-satellite Gravity Recovery And Climate Experiment (GRACE) mission. The paper will also investigate recent GRACE models that are now derived from more than 10 years of data. As these satellite-only models only provide the long and medium wavelength components of the gravity field, the analysis includes an extra-high degree model. EIGEN-6C4 is complete to degree/order 2190 and combines GRACE and GOCE data with terrestrial and altimetry-derived gravity data to improve the determination of the complete Earth's gravity field.

The first three releases of GOCE models were assessed using the GPS-Levelling data in Canada (Ince et al. 2012; Huang and Véronneau 2014). It was suggested that the third release of GOCE models were consistent with the Canadian terrestrial gravity data up to spherical harmonic degree 180 showing evident improvement over the first and second releases of models. Similar assessments have been made in other regions and globally using 1) GPS-Levelling data (Gruber et al. 2011; Janák and Pitoňák 2011; Guimarães et al. 2012; Odera and Fukuda 2013; Godah et al. 2014; Ince et al. 2014; Li et al. 2014; Šprlák et al. 2014; Tocho et al. 2014; Vergos et al. 2014; Voigt and Denker 2014), 2) terrestrial gravity data (Hirt et al. 2011; Guimarães et al. 2012; Rexer et al. 2013; Šprlák et al. 2014; Vergos et al. 2014; Voigt and Denker 2014), 3) deflections of the vertical (Hirt et al. 2011; Voigt and Denker 2014), and 4) topographic forward modelling (Hirt et al. 2012b; Tsoulis and Patlakis 2013).

Assessments of the new releases of GRACE- and GOCE-based models are to understand what new and improved gravity information these models have brought in; what unique contribution each mission has made; how accurate these models are; and how combined models like EIGEN-6C4 have improved determination of the full Earth's gravity field. Answers to these questions are important in order to improve geoid modelling as Canada adopted officially the geoid-based Canadian Geodetic Vertical Datum of 2013 (CGVD2013) in November 2013. This study attempts to address these questions through assessing the recent GRACE and GOCE Release 5 (R5) geopotential models using GPS-Levelling data, astronomic deflections of the vertical and terrestrial gravity data in Canada. Following this section, Section 2 describes the methods followed for the assessments. Section 3 lists the GRACE- and GOCE-based global geopotential models assessed in this report. Section 4 provides details about the independent datasets used in the validation of the GGM. Analysis of the results is presented in Section 5. Finally, Section 6 summaries the study.

2 Methods

2.1 Comparison of Geoid Heights

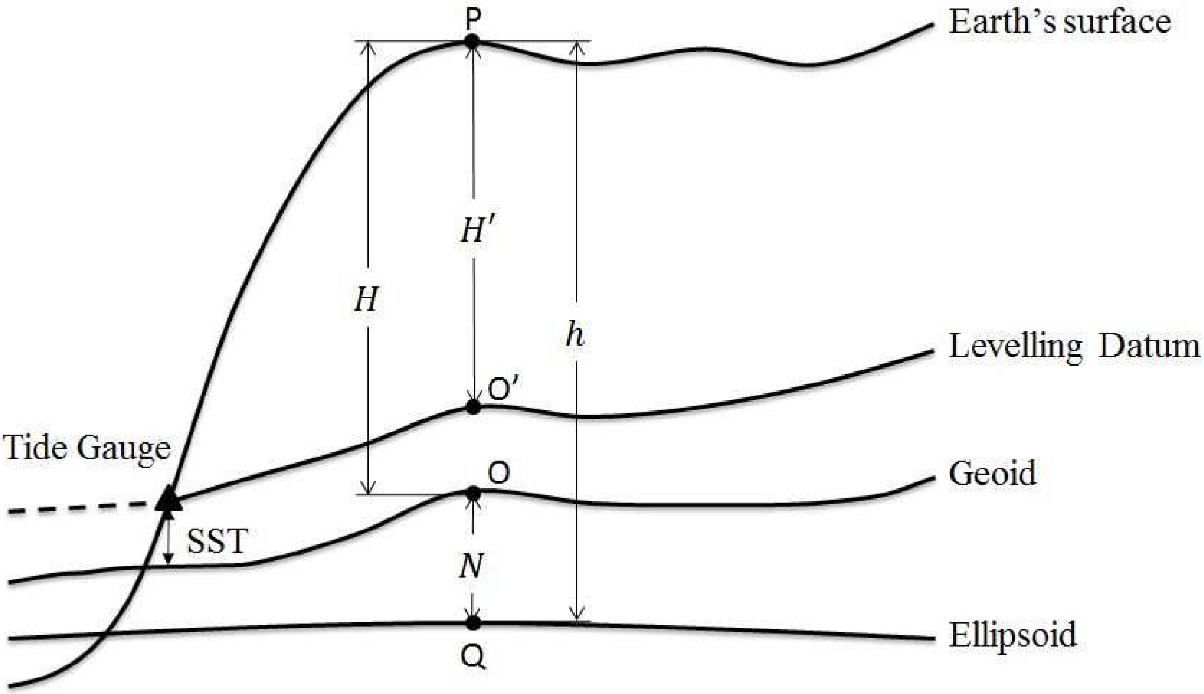

Figure 2.1 Geoid, orthometric and ellipsoidal heights.

Geoid heights N can be calculated by the GPS-measured ellipsoidal heights h and spirit-levelled orthometric heights H at benchmarks. These geometrically-determined geoid heights are independent of the gravimetric-determined geoid heights (see Figure 2.1), providing an ideal method to validate precision of geoid models, i.e.,

$$\epsilon = h - H - N \quad (2.1)$$

The first two terms on the right side of equation (2.1) gives the GPS-Levelling geoid height. Strictly speaking, the determination of precise orthometric heights requires gravity measurements along the leveling line. If we assume that all three heights are errorless, the residual ϵ is negligible, being generally smaller than 1 mm (Jekeli 2000). This is the basic equation for the comparison of GPS-Levelling and gravimetric geoid heights. Considering measurement and modelling errors, the actual residual ϵ can be expressed as

$$\epsilon = \epsilon_{\mathrm{h}} - \epsilon_{\mathrm{H}} - \epsilon_{\mathrm{N}} \quad (2.2)$$

The three terms on the right side of equation (2.2) are errors of the corresponding heights. The ellipsoidal height error ϵ_{h} is considered mostly random while the orthometric height and geoid height often consists of both random and inhomogeneous systematic errors (ϵ_{H}, ϵ_{N}). Figure 2.1 shows that the levelling-determined orthometric height H' can also be biased with respect to the geoid by the mean sea surface topography (SST) as levelling datums are generally defined by the mean sea level at a specific tide gauge. These errors are usually impossible to obtain at individual GPS-Levelling data stations. Instead the error propagation by the least-squares principle is normally used to estimate their standard deviations. The combined GPS-Levelling standard deviation errors provide the base level of residuals for assessment of a geoid model. If they are known, the geoid standard deviation errors can be estimated. Otherwise the comparison can only show relatively statistical geoid improvement from model to model. The latter case applies to this study as the systematic errors of the orthometric heights in Canada are not well known.

The geoid can be determined from regional and global approaches. In regional geoid determination, the geoid height at a point is computed by the remove-compute-restore (RCR) Stokes-Helmert scheme (Huang and Véronneau 2013):

$$N(\Omega) = N_0(\Omega) + N_1(\Omega) + N_{\mathrm{GGM}}(\Omega) + \frac{R}{4\pi\gamma_{\mathrm{E}}} \iint_{\sigma_0} S_{\mathrm{M}}(\psi)[\Delta g(\Omega') - \Delta g_{\mathrm{GGM}}(\Omega')]d\sigma + \delta N \quad (2.3)$$

where Ω and Ω' are the geocentric angles denoting the geodetic longitude and latitude pairs (λ, φ) and (λ', φ') of the computation and integration points, respectively. The term N_0 accounts for mass and potential differences between the Earth and the reference ellipsoid (see Equation 2-182, Heiskanen and Moritz 1967). The term N_1 corrects for misalignment between the Earth's centre of mass and the origin of the reference coordinate system (see Equation 2-176b, Heiskanen and Moritz 1967). N_{GGM} and Δg_{GGM} represent the Helmert geoid height and gravity anomaly synthesized from a GGM and spherical harmonic forms of the digital elevation model (DEM). The spherical harmonic DEM is used to transform the two parameters above from real space to Helmert's space to realize the RCR scheme in Helmert's space (Huang and Véronneau 2013). S_{M} is the modified degree-banded kernel function. ψ is the spherical angle between the point of computation and an integration point. Δg is the surface Helmert gravity anomaly on the geoid derived from ground and airborne gravity and topographical data. R is the mean radius of the Earth. γ_{E} is the normal gravity on the reference ellipsoid. The symbols σ_0 and $d\sigma$ stand for the local domain and the surface area element on a unit sphere, respectively. The Stokes integral gives the geoid residual in a spherical approximation, which is accurate enough to achieve centimeter accuracy when a GRACE and GOCE satellite GGM model is used in the RCR scheme. Finally, the last term δN is the primary indirect effect which transforms the Helmert co-geoid height to the geoid height.

The modified degree-banded Stokes kernel function ($S_M(\psi)$) can be expressed as (Huang and Véronneau 2013):

$$S_{\mathrm{M}}(\psi) = \sum_{n=2}^{nx} \alpha_n(L) \frac{2n+1}{n-1} P_n(cos\psi) \quad (2.4)$$

where nx is the upper limit of the spherical harmonic degree and corresponds to the spectral content of the terrestrial gravity data. α_n are the spectral transfer coefficients of spherical harmonic degree n, and P_n are the Legendre's polynomials. Figure 2.2 shows α_n for three modification degrees L (180, 210 and 240) which determine how the GGM and terrestrial gravity anomalies are combined together. Figure 2.2 (left) shows the low spherical harmonic degrees of α_n. The spectral transition has a 60-degree bandwidth, where α_n increase from 0 at degree $L - 60$ to 1 at degree L. The higher is the modification of degree L, the more satellite gravity data is introduced into the solution, replacing the corresponding components of the terrestrial gravity anomalies. This substitution can improve a geoid model when the GGM components are more accurate than the terrestrial gravity components replaced, and vice versa (Huang and Véronneau 2015). Figure 2.2 (right) shows the high spherical harmonic degrees of α_n. The spectral transition bandwidth is 120 degrees, for which α_n decrease from 1 at degree 5400 to 0 at degree 5520 for the three cases. Degree 5400 corresponds to the 2' by 2' spatial resolution of the terrestrial gravity data. Thus, for the spherical harmonic degrees between degrees L and 5400, the terrestrial gravity data contribute entirely to the geoid model as $\alpha_n = 1$.

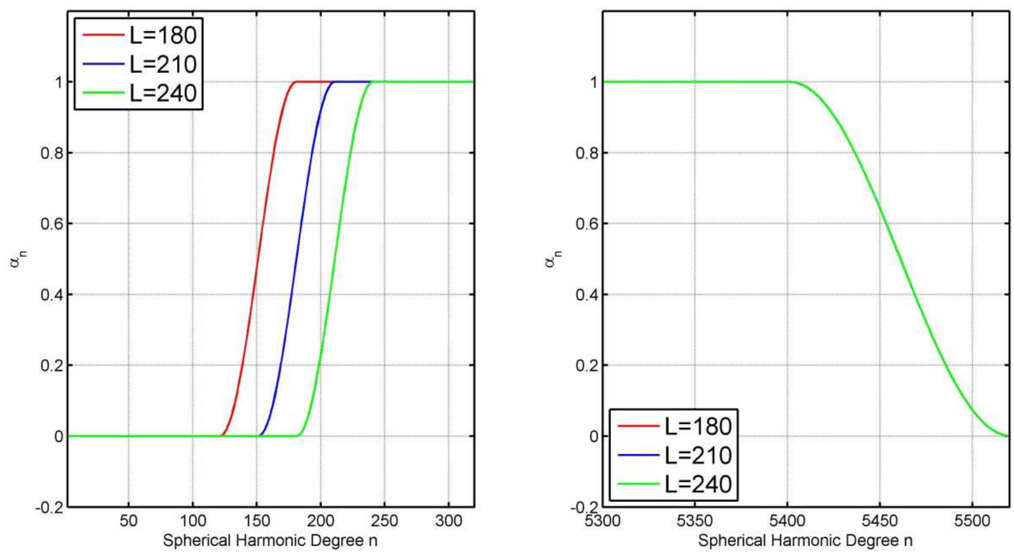

Figure 2.2 The spectral transfer coefficients α_n of the low (left) and high (right) spherical harmonic degrees for modification degrees $L = 180, 210, 240$. Note: the curves for L = 180 and 210 are the same as L = 240 on the right graph.

At the global scale, the Earth's gravity field is generally depicted by a spherical harmonic expansion. The geoid height can then be computed from a GGM as

$$N_{n_{\max}}(\Omega) = N_0(\Omega) + N_1(\Omega) + \frac{GM}{r_{\mathrm{E}}\gamma_{\mathrm{E}}} \sum_{n=2}^{n_{\max}} \left(\frac{a}{r_{\mathrm{E}}}\right)^n \sum_{m=0}^{n} \overline{C}_{nm} \overline{Y}_{nm}(\Omega) + C_{\mathrm{T}}(\Omega) \quad (2.5)$$

The third term represents the sum of the spherical harmonic components of the geoid synthesized from the GGM. The pair of (GM, a) are the scaling geocentric gravitational constant and radius of the GGM, respectively. $\overline{C}_{nm}$ are the fully normalized spherical harmonic geopotential coefficients that have been reduced by the even harmonic coefficients of the reference field. $\overline{Y}_{nm}$ are the fully normalized spherical harmonic functions of degree n and order m. The last term is a correction for the topographical effect (see Appendix A).

2.2 Comparison of Astronomic Deflections of the Vertical

A deflection of the vertical according to Helmert's projection is the angle at point P between the gravity vector and the normal to the reference ellipsoid. The deflection is composed of a north-south component (ξ) and east-west component (η). They can be determined by astronomic and geodetic observations to the 2nd-order term (Jekeli 1999):

$$\begin{aligned} \xi &= \Phi - \phi + \frac{1}{2}\eta^2 \tan(\phi) \\ \eta &= (\Lambda - \lambda)\cos\phi \end{aligned} \qquad \text{(2.6a and 2.6b)}$$

where the pair (Φ, Λ) are the astronomic latitude and longitude, and the pair (ϕ, λ) are the geodetic latitude and longitude.

In this study, astronomic deflections of the vertical are compared to the corresponding deflections derived from global and regional geoid models. Given gravimetric height anomalies, we can compute the deflections of the vertical according to Helmert's projection by (see 8-9, Heiskanen and Moritz 1967):

$$\begin{aligned} \xi &= -\frac{1}{R}\frac{\partial \varsigma}{\partial \phi} - \frac{\Delta g}{\gamma}\frac{1}{R}\frac{\partial H}{\partial \phi} + 0.17'' H_{\text{km}} \sin 2\phi \\ \eta &= -\frac{1}{R\cos\phi}\frac{\partial \varsigma}{\partial \lambda} - \frac{\Delta g}{\gamma}\frac{1}{R\cos\phi}\frac{\partial H}{\partial \lambda} \end{aligned} \qquad \text{(2.7a and 2.7b)}$$

where ς is the height anomaly on the Earth's surface, and can be computed from the geoid height by

$$\varsigma = N - \frac{\Delta g_{\text{B}}}{\overline{\gamma}} H \qquad \text{(2.8)}$$

Δg is the free-air gravity anomaly, H is the orthometric height, and Δg_{B} is the Bouguer gravity anomaly. The height anomaly ς needs be transferred to the observation point level for evaluating deflections of vertical. The first terms of Equations (2.7a and 2.7b) only give approximate deflection values, and the second terms of Equations (2.7a and 2.7b) are corrections for the transfer to the observation point level to meet the theoretical requirement. The third term in Eq. (2.7a) is the correction for the normal curvature of the plumb line which converts the north-south component to the corresponding component defined in Equation (2.6a). The deflection at a point is numerically computed from the derivative of the closest nine grid points of a geoid model and the DEM. In Canada, geoid models have a standard resolution of 2' by 2' (~3.6 km in the north-south direction). This results in having modelled deflections of the vertical that do not contain spectral components at the scale less than 2'. Therefore, the differences between the observed and modelled deflections are affected by the omission errors in the geoid models. In this study, we do not estimate this omission error as all regional geoid models are subject to the same one. The objective of study is to assess relative improvement of GOCE models from one release to next one. However, the omission error could be taken into consideration using the residual terrain modelling technique in future studies as demonstrated by Hirt et al (2010) on an European dataset.

2.3 Comparison of Gravity Anomalies

The gravity anomalies can be computed from a GGM by the following formula (Heiskanen and Moritz, 1967):

$$\Delta g(\Omega, r_{\mathrm{S}}) = -\left.\frac{\partial T(\Omega, r)}{\partial h}\right|_{r=r_{\mathrm{E}}} + \frac{1}{\gamma}\frac{\partial \gamma}{\partial h} T(\Omega, r_{\mathrm{E}}) + UC \qquad (2.9)$$

where

$$T\ (\Omega, r) = \frac{GM}{r}\sum_{n=2}^{nx}\left(\frac{a}{r}\right)^{n}\sum_{m=0}^{n}\overline{C}_{nm}\overline{Y}_{nm}(\Omega) \qquad (2.10)$$

These synthesized anomalies can be compared to the measured gravity anomalies. The routine 'Harmonic_synth.f' (version 05/01/2006, isw=50, 03 and 06) provided by the National Geospatial-intelligence Agency (NGA) was used to compute the free-air gravity anomaly on the Earth's surface at the observed gravity points.

In the computation, the ellipsoidal height at each point is computed by adding the CGG2013 geoid height to the orthometric height, which is corrected by a bias of -8 cm, representing the mean separation between Canada's old datum (CGVD28) and new datum (CGVD2013). In a second step, the ellipsoidal height is used to compute the second-order upward continuation correction *UC* to the free-air anomaly evaluated on the reference ellipsoid. The zero-degree term due to the difference between the geopotential constants GM of GGM and GRS80 is 0.144 mGal in absolute value and is added to the synthesized free-air anomalies. Input parameters were set to produce point values in the tide-free system with reference to GRS80 (Moritz 1980).

3 Global Geopotential Models

Table 3.1 Global geopotential models.

Model	**Max Degree**	**Data Sources**	**Authors**
GGM05S	180	GRACE (2003-2013) and SLR	Tapley et al. 2013
ITSG-Grace2014s	200	GRACE (2003-2013)	Mayer-Gürr et al. 2014
TIM-R4	250	GOCE	Pail et al. 2011
DIR-R4	260	Lageos, GRACE, GOCE	Bruinsma et al 2013
TIM-R5	280	GOCE	Brookmann et al. 2014
DIR-R5	300	Lageos, GRACE, GOCE	Bruinsma et al. 2014
EGM2008	2190	GRACE, Gravity, Altimetry	Pavlis et al. 2012
EIGEN-6C4	2190	GRACE, GOCE, Gravity, Altimetry	Förste et al. 2014

In this study, we assess seven GRACE and GOCE GGMs. These models are listed in Table 3.1. They include two recent GRACE models: GGM05S (Tapley et al. 2013) and ITSG-Grace2014s (Mayer-Gürr et al 2014); two GOCE R5 models: TIM-R5 (Brockmann et al. 2014) and DIR-R5 (Bruinsma et al. 2014); two GOCE R4 models: TIM-R4 (Pail et al. 2011) and DIR-R4 (Bruinsma et al. 2013); and one extra-high spherical harmonic model: EIGEN-6C4 (Förste et al. 2014). EIGEN-6C4 combines the four main types of gravity data (GRACE, GOCE, Terrestrial and altimetry). EGM2008 (Pavlis et al. 2012) is also included as a baseline for the comparisons. Among these GGMs, TIM-R5, DIR-R5 and EIGEN-6C4 include GOCE data for its entire mission.

4 Data

4.1 GPS and Levelling on Benchmarks

There are 2,668 benchmarks (BMs) observed by spirit levelling and GPS spreading through five independent levelling networks for this study. These networks encompass the Canadian mainland (CA) with 2449 BMs, the provinces of Newfoundland (NFLD) with 113 BMs and Prince Edward Island (PEI) with 18 BMs, as well as Anticosti Island (AI), located in the Gulf of St-Lawrence, with 15 BMs, and Vancouver Island (VI) with 73 BMs on the west coast. The mainland network includes few benchmarks in Alaska as a levelling loop in the Yukon Territory goes within the USA. The orthometric heights are from the Sept12 adjustments. These are minimum constraint adjustments. For example, the mainland network is constrained to a single benchmark in Halifax, Nova Scotia. The datum at this station is the equipotential surface $W_0 = 62636856 m^2 s^{-2}$ (definition of CGVD2013), determined by $(\mathrm{h} - \mathrm{N}) * \bar{\mathrm{g}}$ where N is from CGG2010 transformed to the above mentioned equipotential surface. The GPS ellipsoidal heights are from two national adjustments: version 3.3 for the GPS survey between 1986 and 1993 and version 5.3.1 for the GPS survey after 1993 (Craymer personal communication 2012). All the ellipsoidal heights are in ITRF2008 and transformed to epoch 2010.0.

4.2 Astronomic Deflections of the Vertical

In Canada, the astronomic observations were collected between 1910 and 1975. The geodetic coordinates were derived by traditional angular and distance measurements, and transformed into ITRF93. Figure 4.1 shows the distribution of the 939 astronomical deflections of the vertical in Canada while Table 4.1 provides some statistical information. These deflections are the same ones that were used in the evaluation of EGM2008 (Huang and Véronneau 2009).They have estimated accuracy between 0.3 and 0.5 arcsec. The second order term in Equation (2.6a), which is smaller than 0.005 arcsec for all the stations, is negligible.

Table 4.1 Statistics of deflections of the vertical in arcsec.

	Number	**Min**	**Max**	**Mean**	**StdDev**	**R.M.S.**
ξ (north-south)	939	-23.41	17.88	0.21	4.50	4.51
η (east-west)	939	-22.39	24.35	-0.23	6.14	6.14

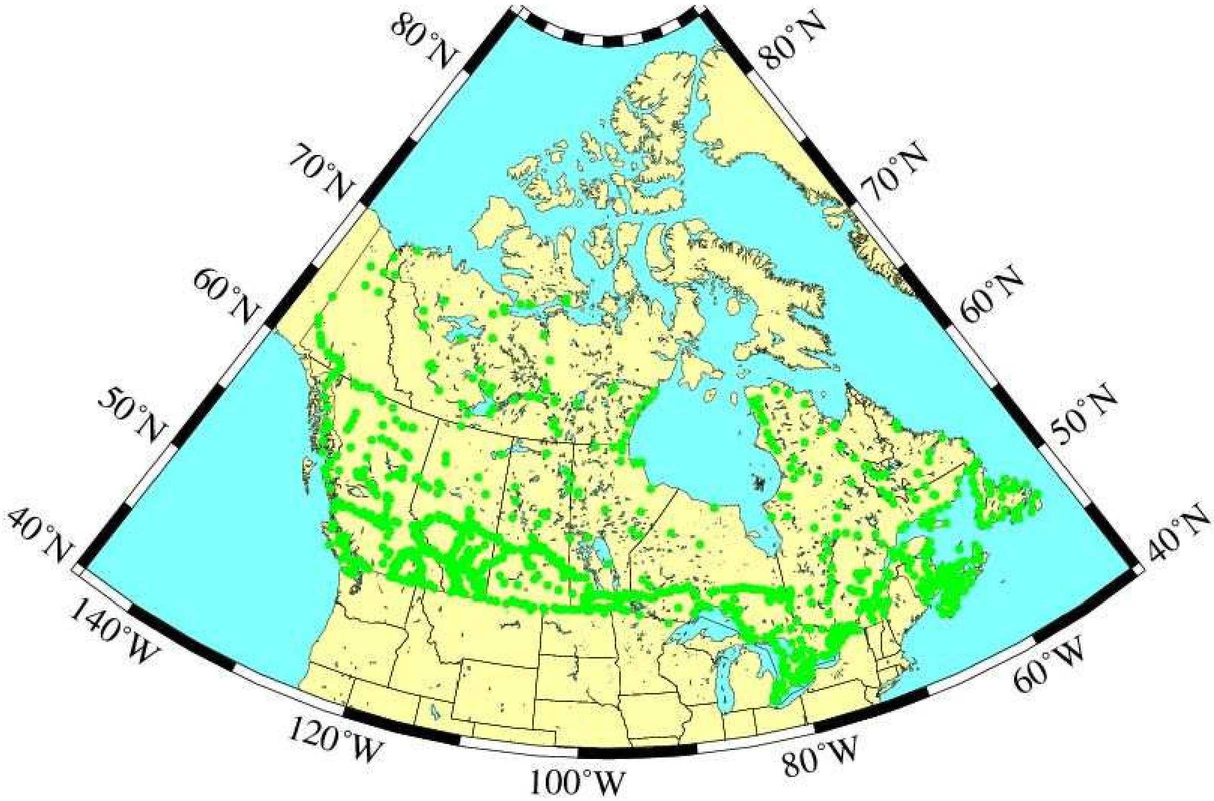

Figure 4.1 Location of the 939 astronomic deflections of the vertical in Canada.

4.3 Gravity Anomalies

In Canada, gravity data include a collection of gravity observations on land, ice caps, sea and lake surfaces (ship and ice), sea and lake bottoms, and in the air (airborne). About 98 percent of the observations were collected over the last 50 years covering entirely Canada and neighboring oceans. There are some 750,000 Canadian gravity measurements in the gravity database (CGDB). Each record essentially contains the station unique number, latitude, longitude, gravity, error estimate, observation year, etc. The accuracy of the derived free-air gravity anomalies (GRS80) varies across Canada depending on the type of instruments, platforms, height reductions, etc. The estimates of their errors range from 0.01 to 10.01 mGal with a mean of 1.88 mGal. Among these observations, the overall accuracy of land gravity observation is the best. Table 4.2 shows a statistical description of the free-air gravity anomalies along their error estimates and elevations. The error for the anomalies is the combination of the errors coming from gravity and elevation measurements, the elevation being the dominant error source. Figure 4.2 depicts the error of the gravity anomalies in Canada. One can observe that the error estimates are smaller than 1 mGal over most of the Canadian territory. The larger errors can be seen over Baffin Island, Northwest Territories, northern Quebec and southern British Colombia. The same land gravity data set was used for the evaluation of EGM2008 (Huang and Véronneau 2009); though, the gravity database now includes an additional ~15,000 measurements.

Table 4.2 Statistical description of the 231,079 free-air gravity anomalies over land.

Data	Min	Max	Mean	StdDev	R.M.S.
Free-air anomalies (mGal)	-183.62	393.31	-9.99	28.73	30.42
Error standard deviations (mGal)	0.00	9.26	0.83	0.72	1.10

Elevations (m)	-4	4945	382	361	526

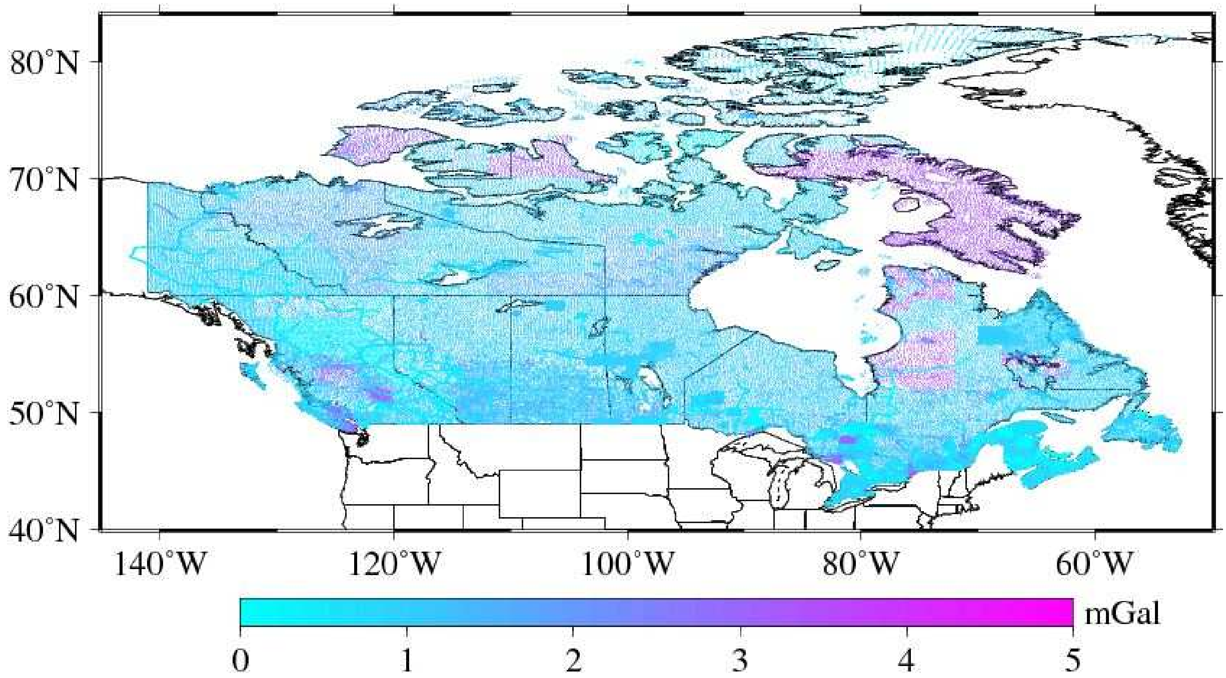

Figure 4.2 Distribution of 231,079 land gravity points. The colour scale indicates the magnitude of the error estimates. Note: The upper limit of the colour scale does not represent the maximum error estimate; the error values greater than 5 mGal are shown as the upper limit color.

The atmospheric correction in GRS80 (Moritz 1980) was applied to the free-air anomalies using the following formula:

$$Dg_{\mathrm{A}} = 0.87e^{-0.116H_{\mathrm{km}}^{1.047}}$$

where H_{km} is the orthometric height in kilometer. The atmospheric correction is in mGal.

5 Assessments and Results

5.1 Using GPS and Levelling Data

The Canadian Geodetic Survey computed a series of gravimetric geoid models according to Equations (2.3) and (2.4) using a range of modification degrees starting at degree L=120. The gravimetric geoid models used the same terrestrial gravity data and Digital Elevation Models as CGG2013 so that the resulting models differ only by the underlying satellite model and the degree of modification. Geoid heights are interpolated at the GPS-Levelling stations from each gravimetric geoid model using the bi-linear method. The gravimetric geoid heights are compared with the GPS-Levelling geoid heights according to Equation (2.1). The standard deviation of the residuals ($h - H - N$) is used to characterize the level of the residuals because it is not affected by the datum bias of the levelling network. The results are shown in Figures 5.1 and 5.2 for mainland Canada (CA) and five sub-regions: the Yukon Territory (YK), northern British Columbia (NBC), the Great Lakes (GL), the Maritimes (MT) and Newfoundland (NFLD). These five sub-regions correspond to relatively large geoid updates from GRACE and GOCE models as shown in Figures 5.3 and 5.4. In addition, EIGEN-6C4 has also been used to compute a geoid model according to Equation (2.5). The C_{T} term is computed to degree/order 2190 using the spherical harmonic DEM models complete to degree/order 2700 provided by the US National Geodetic Survey. They are based on a mean 1 arcmin grid averaged from the 30 arcsec SRTM grid (Wang 2009). The GPS-Levelling comparisons are also done against EIGEN-6C4 and CGG2013 (see Figures 5.1 and 5.2).

A progressive improvement can be seen from GRACE-only, GOCE-based R4 and R5 models in terms of the GPS-Levelling comparisons. Firstly, both GRACE models improve from $L = 120$ to 150, and deteriorate from $L = 150$ to 180. GGM05S deteriorates more rapidly than the ITSG-Grace2014s. The fact that both GRACE models are un-constrained, and use the approximately same data period suggests that the latter is better than the former beyond degree 150. Secondly, GOCE-only model TIM-R4 performs significantly better than ITSG-Grace2014s for $L = 180$ and higher. This improvement over the GRACE model can be attributed to GOCE contribution, and partly to Kaula's regularization applied to TIM-R4 beyond degree 180. The DIR-R4 model gives similar results, and further confirms the GOCE contribution. Thirdly, GOCE-only model TIM-R5 performs significantly better than TIM-R4 beyond degree 180, and maintains the same level of residuals until degree 240. The better and steady performance of TIM-R5 from $L = 180$ can be attributed to the last stage of GOCE observation at the lower orbits, and partly due to Kaula's regularization applied to TIM-R5 beyond degree 200. The DIR-R5 model again confirms the improvement from the last stage of GOCE observation. One exception is found in Newfoundland where DIR-R4 (also CGG2013) outperforms DIR-R5 being likely attributed to the striping error when combining the GRACE models in the DIR solutions (see more discussions later in this section). Note that the levelling lines in Newfoundland extend from 150 to 380 km in the north-south direction and from 150 to 350 km in the east-west direction. These levelling lines are long enough in assessing GOCE models.

Furthermore comparing the performances of TIM-R5 and DIR-R5 suggests that the GOCE-only model is almost equivalent to the combined GRACE and GOCE model DIR-R5 in terms of the residual levels of the GPS-Levelling comparisons. DIR-R5 performs better for mainland Canada, the Yukon Territory, northern British Columbia, the Great Lakes region, but worse for the Maritimes and Newfoundland than TIM-R5. These results do not allow us draw a simple and general conclusion on which of the two R5 models is better in Canada. Overall, we can conclude that the best modification degree is $L = 150$ for the GRACE-only models and $L = 200$ for the GOCE-based models (R5).

CGG2013 is included in the analysis to serve as a baseline to assess improvements in the R5 models. CGG2013 uses the low-degree components of EIGEN-6C3stat (L = 180), which is based on a GOCE-based R4 model by the DIR approach (Förste et al., 2013). For $L = 180$ in Figures 5.1 and 5.2, CGG2013 maintains the same level of residuals as the geoid models based on TIM-R5 and DIR-R5 except for the Maritimes region where a smaller standard deviation is observed for both TIM-R4 and TIM-R5. The two geoid models using TIM-R5 and DIR-R5 for $L = 200$ show slightly lower residual levels than CGG2013. This indicates that these two GOCE models bring slightly more precise signal components into the two resulting geoid models than EIGEN-6C3stat in CGG2013. The GOCE signals allow improvement over the terrestrial gravity data for the frequency band between 120 and 200 (L = 180 to 200). For instance, TIM-R5 and DIR-R5 based geoid models modified to degree $L = 200$ outperform CGG2013 by about 0.5 cm along the GPS-Levelling line (26 BMs) that crosses the vertical stripes in the central Quebec (see Figures 5.3 and 5.4).

The geoid updates to CGG2013 by both TIM-R5 and DIR-R5 display a pattern of the GRACE-like striping error as shown in Figures 5.3 and 5.4 over eastern Canada. We have plotted differences between a number of TIM-4 and TIM-5 based regional geoid models (not shown here). They do not show a striping pattern like Figures 5.3 and 5.4 as Brockmann et al. (2014) have shown. This suggests that the GRACE model is the source of the striping pattern. The difference map between DIR-R4 and DIR-R5 by Bruinsma et al. (2014) has also shown the trace of the striping pattern. Thus the striping pattern in Figure

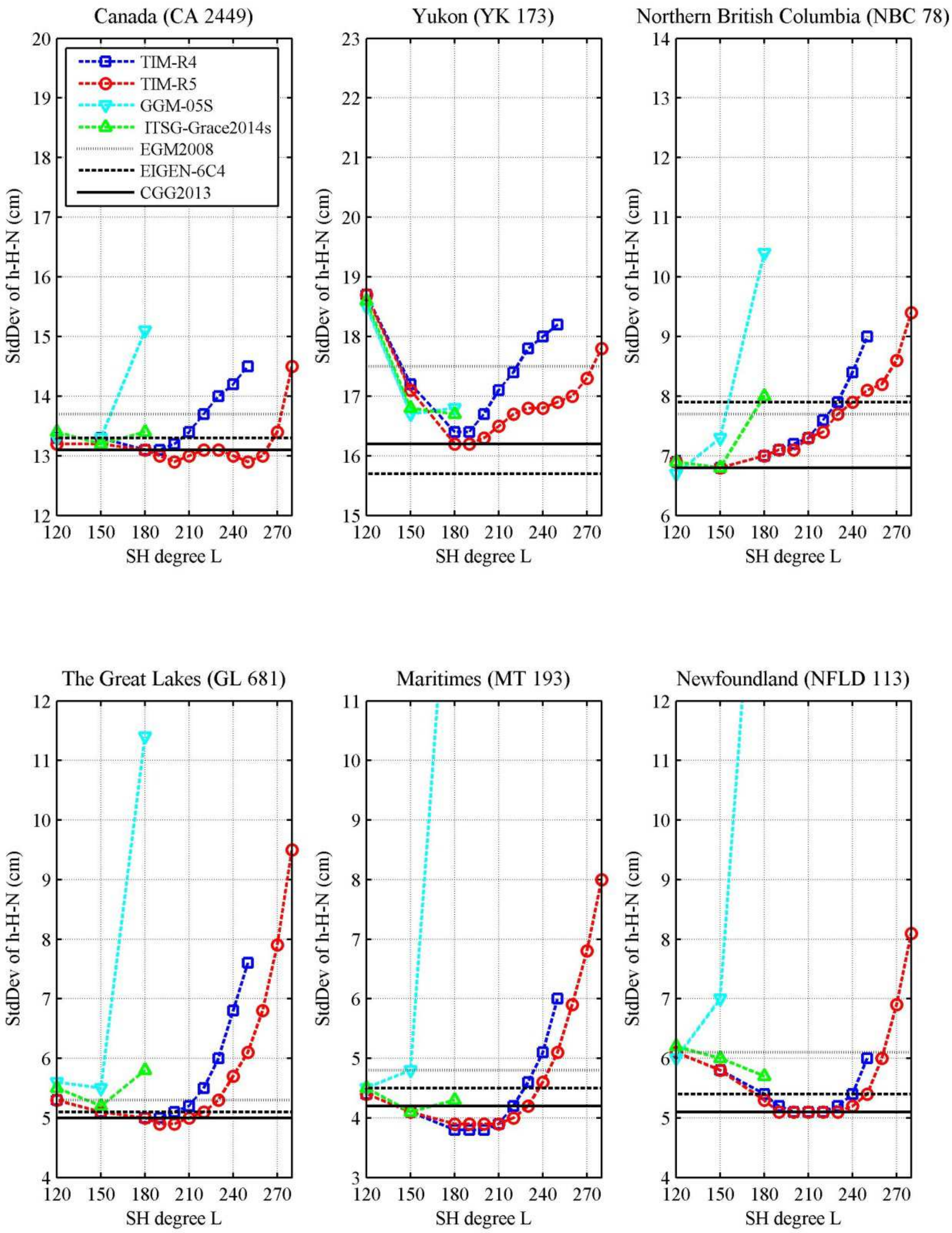

Figure 5.1 The standard deviations of $(h - H - N)$ for mainland Canada, and five sub-regions using recent GRACE and **GOCE-only** (TIM-R4 and -R5) GGMs (Unit: cm). The number of GPS-Levelling points for each region is given between parentheses. The range of the vertical axis is 8 cm.

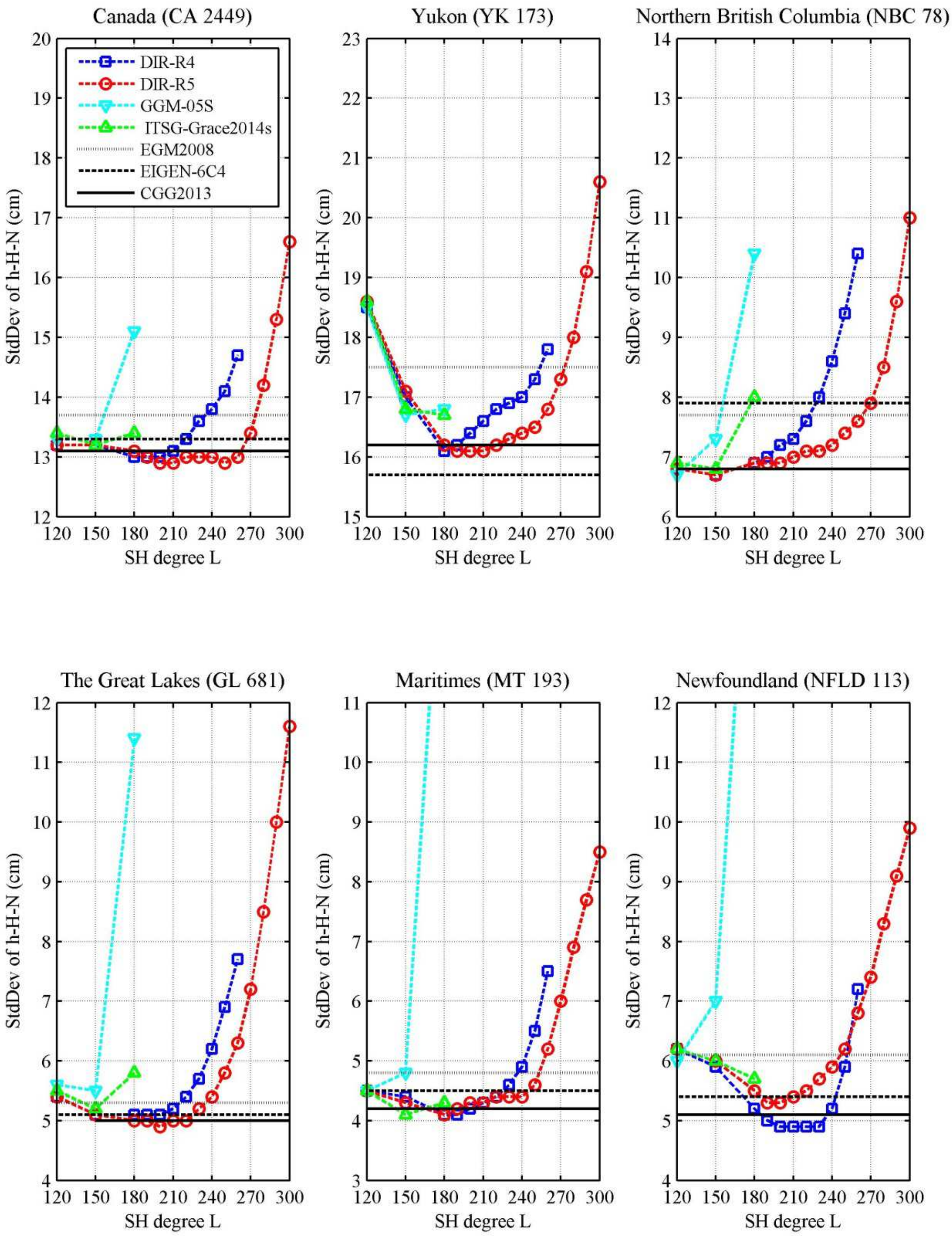

Figure 5.2 The standard deviations of $(h - H - N)$ for mainland Canada, and five sub-regions using recent GRACE and **combined GRACE and GOCE** (DIR-R4 and –R5) GGMs (Unit: cm). The number of GPS-Levelling points for each area is given between parentheses. The range of the vertical axis is 8 cm.

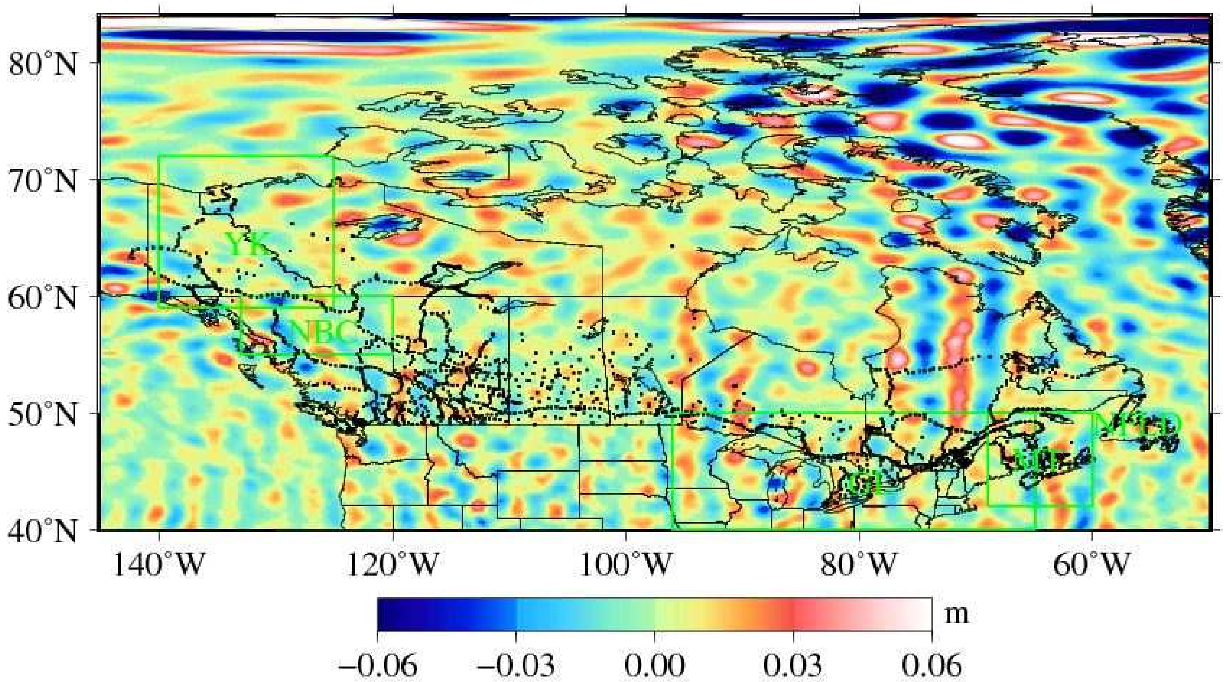

Figure 5.3 The geoid differences between M023 (TIM-R5, $L = 200$) and CGG2013. The black squares mark the GPS-Leveling stations.

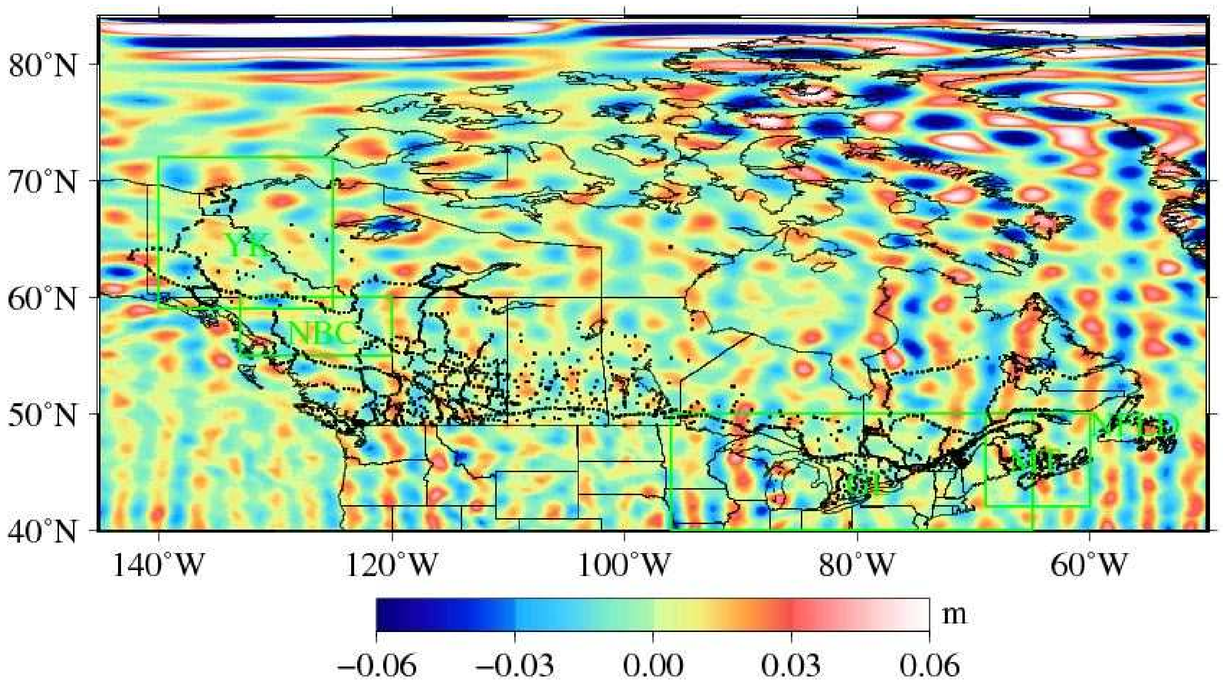

Figure 5.4 The geoid differences between M035 (DIR-R5, $L = 200$) and CGG2013. The black squares mark the GPS-Leveling stations.

5.3 is considered from CGG2013 which indirectly uses the GRACE model via EIGEN-6C3stat, while the striping pattern in Figure 5.4 comes from both CGG2013 (indirectly based on DIR-R4) and DIR-R5. The update from DIR-R5 improves CGG2013 in central Quebec on one hand, but worsens CGG2013 in Newfoundland on the other hand. This inconsistent performance appears due to the method for combination of GRACE models into the DIR models.

CGG2013 outperforms EIGEN-6C4 in mainland Canada and for four out of five sub-regions mostly due to its higher spatial resolution. This suggests that the omission error is still a limitation factor for EIGEN-6C4 in modelling the geoid in Canada regardless that it combines the latest gravity information from all sources. The residual levels of EGM2008 are also shown in Figures 5.1 and 5.2, and are generally higher than the ones for the EIGEN-6C4 geoid. Over the Canadian land, both EGM2008 and EIGEN-6C4 are based on the same terrestrial gravity data. The improvement from EIGEN-6C4 is considered primarily due to the use of the GOCE model. Note that we have used the EGM2008 GRS80 geoid undulation grid for this study, which is transformed from the 1 by 1 arcmin WGS84 geoid undulation grid by the NGA (http://earth-info.nga.mil/GandG/wgs84/gravitymod/egm2008/egm08_wgs84.html). In the meantime, we have computed an EGM2008 geoid undulation grid using the same spherical harmonic DEM as the one for EIGEN-6C4. The statistical results of the GPS-Levelling comparison only differ slightly (0 mm for GL, 1 mm for CA, NBC and MT, and 2 mm for YK in standard deviation) for the two EGM2008 geoid undulation grids even though the differences between them can reach decimeters at the extreme cases, mostly over high mountains where there are no GPS-Levelling data.

The residual levels vary from region to region with the lowest level in the Maritimes and the highest level in the Yukon Territory reflecting the sum of errors from the geoid models and GPS-Levelling data. The GPS ellipsoidal heights generally have a precision better than 2 cm at most of the stations, but the error can be larger than 10 cm for the surveys conducted before 1994. The levelling orthometric heights are as precise as a few millimeters within a few kilometers, but contain a systematic error slope of about 30 cm from the eastern to western coasts. A simple four-parameter fit to remove the error slope reduces the residual level of CGG2013 in mainland Canada from 13.1 cm to 7.3 cm. The smaller a region is, the less the effect of the error slope. For instances, the levels of residuals in the Great Lakes and Maritimes regions are about 4-5 cm, which are less affected by the error slope and more reflect the total random errors. A similar level of residuals is also observed in Newfoundland as well as other regions of similar sizes not included in this study. These results imply that the GOCE components of the geoid models are accurate to better than 4-5 cm. The high level of residuals in the Yukon Territory is mostly related to the poor closure of the large levelling loops and instability of the benchmarks in this remote region.

5.2 Using Deflections of the Vertical Data

Deflections of the vertical have been determined according to the method described in Section 2.2 from eight geoid models. The results of the comparison between the model-derived deflections and the astronomic deflections are shown in Table 5.1. The two global models (EGM2008 and EIGEN-6C4) are chosen to validate the GOCE contribution to the global geopotential modelling while four regional geoid models (M04, M13, M23 and M35) with modification degree $L = 200$ are selected to validate the improvement of the R5 models over the R4 models. The M58 model is selected to determine if EIGEN-6C4 performs better than EIGEN-6C3stat which underlies CGG2013 (L = 180).

The EGM2008 model gives a slightly lower residual level than the EIGEN-6C4 model for both the north-south and east-west components (see Table 5.1). The six regional geoid models show the almost same levels of residuals, a standard deviation of 1.23 arcsec for the north-south component and 1.58 arcsec for the east-west component. The standard deviations represent geoid slopes of 6.0 cm and 7.7 cm over a 10-k m distance. Error slopes of this magnitude are not observed in the geoid models when compared to

GPS/Levelling data. This indicates that the astronomical deflections may not be as accurate as estimated, the transfer from the geoid to the topography may introduce errors and/or the resolution of the models is not high enough. The residual levels could be significantly reduced by the residual terrain modelling (RTM) technique as it is shown in Hirt et al. (2010).

To help understand these results, differences of the model-predicted deflections have also been computed from four pairs of geoid models and shown in Table 5.2. They represent deflection corrections of the R5 models to the previous release. The level of the corrections is lower than 0.3 arcsec for the two global models and 0.1 arcsec for the six regional models. It suggests that the deflections must be accurate to better than 0.1 arcsec to validate improvement from the R5 GOCE models. The accuracy of the astronomic deflections is about 0.3 to 0.5 arcsec, and is not accurate enough to validate the improvement from the R5 models. In Table 5.1, the two global models give larger residual levels than the six regional models most likely due to the omission errors of the global models.

Table 5.1 Differences between the geoid model-predicted and astronomic deflections of the vertical at 939 stations (Unit: arcsec).

			ξ (north-south)				η (east-west)			
Geoid Model	**GGM**	**L**	**Min**	**Max**	**Mean**	**StdDev**	**Min**	**Max**	**Mean**	**StdDev**
EGM2008			-9.56	9.94	0.03	1.51	-11.63	7.98	0.17	1.81
EIGEN6C4			-8.51	9.98	0.01	1.55	-11.38	8.38	0.17	1.87
M04	TIM-R4	200	-5.21	9.80	0.05	1.23	-12.94	7.54	0.21	1.58
M23	TIM-R5	200	-5.22	9.75	0.06	1.22	-12.93	7.45	0.22	1.58
M13	DIR-R4	200	-5.23	9.80	0.06	1.23	-12.90	7.54	0.21	1.58
M35	DIR-R5	200	-5.26	9.76	0.06	1.23	-12.87	7.46	0.22	1.58
CGG2013	EIGEN-6C3stat	180	-5.23	9.85	0.06	1.23	-12.92	7.46	0.21	1.58
M58	EIGEN6C4	200	-5.24	9.85	0.06	1.23	-12.89	7.38	0.22	1.58

Table 5.2 Differences of the geoid model-predicted deflections of the vertical at 939 stations (Unit: arcsec).

	ξ (north-south)				η (east-west)			
Model Pair	**Min**	**Max**	**Mean**	**StdDev**	**Min**	**Max**	**Mean**	**StdDev**
EIGEN-6C4 - EGM2008	-1.38	1.40	-0.02	0.24	-1.71	2.00	0.00	0.29
M23 - M04	-0.16	0.16	0.00	0.05	-0.22	0.23	0.00	0.07
M35 - M13	-0.15	0.15	0.00	0.05	-0.22	0.26	0.01	0.08
M58 - CGG2013	-0.18	0.25	0.00	0.05	-0.24	0.27	0.00	0.08

Note that the residual values for EGM2008 in Table 5.1 are smaller than the previous estimated values (Huang and Véronneau 2009). This is mainly because of the use of the Canadian Digital Elevation Data (http://www.nrcan.gc.ca/earth-sciences/geography/atlas-canada/free-data/16894#geobase) which replaced the spherical harmonic DEM provided by NGA for EIGEN-6C4 and EGM2008. In addition, the two additional terrain-related terms in Equation (2.7) are now considered. These two terms can reach up to 2 arcsec with an RMS of 0.2 arcsec at the 939 stations. Also, the statistics presented in 2009 excluded nine stations that did not have proper station identification.

5.3 Using Gravity Data

Gravity comparisons are only limited to the two extra high degree models EGM2008 and EIGEN-6C4 which have significantly smaller omission errors than the satellite-only models due to the use of terrestrial gravity data. Both models directly or indirectly use the same land gravity data in Canada for high-degree components beyond the satellite signal. The latter contains upgraded GRACE signals with respect to the GRACE signals that are included in EGM2008, and GOCE signals to higher spherical harmonic degree and order, and may improve over the former if the new satellite signals are more accurate than the corresponding terrestrial components in EGM2008.

The free-air gravity anomalies have been synthesized from EGM2008 and EIGEN-6C4, and compared to the free-air gravity anomalies at the land gravity points, respectively. The differences are given in Table 5.3 and Figures 5.5 and 5.6. Difference levels for both models are similar. In other words, these gravity comparisons do not show the improvement from EIGEN-6C4 over EGM2008. However they have confirmed that the GOCE components in EIGEN-6C4 agree with the corresponding terrestrial components in EGM2008 to the error level of the land data. The differences of the free-air anomalies synthesized from EIGEN-6C4 and EGM2008 are also shown in Table 5.3 and Figure 5.7. The RMS of the differences is 0.71 mGal that is close to the mean error 0.82 mGal of the land data shown in Table 4.2. In other words, the error level in the land data is too high to resolve the improvement of EIGEN-6C4 over EGM2008. Furthermore, both GGMs are dependent of the land gravity data. EGM2008 depends more than EIGEN-6C4 on the land gravity data, therefore tends to agree better with them.

Table 5.3 Differences between the free-air gravity anomalies and the gravity anomalies synthesized from EGM2008 and EIGEN-6C4 at 231,079 land points, respectively (the first two rows). Differences between free-air anomalies synthesized from the two GGMs are also included (the third row). Unit: mGal.

Model	**Min**	**Max**	**Mean**	**StdDev**
EGM2008	-176.85	175.62	-1.58	13.33
EIGEN-6C4	-177.15	175.53	-1.60	13.37
EIGEN-6C4 – EGM2008	-12.48	10.78	0.02	0.71

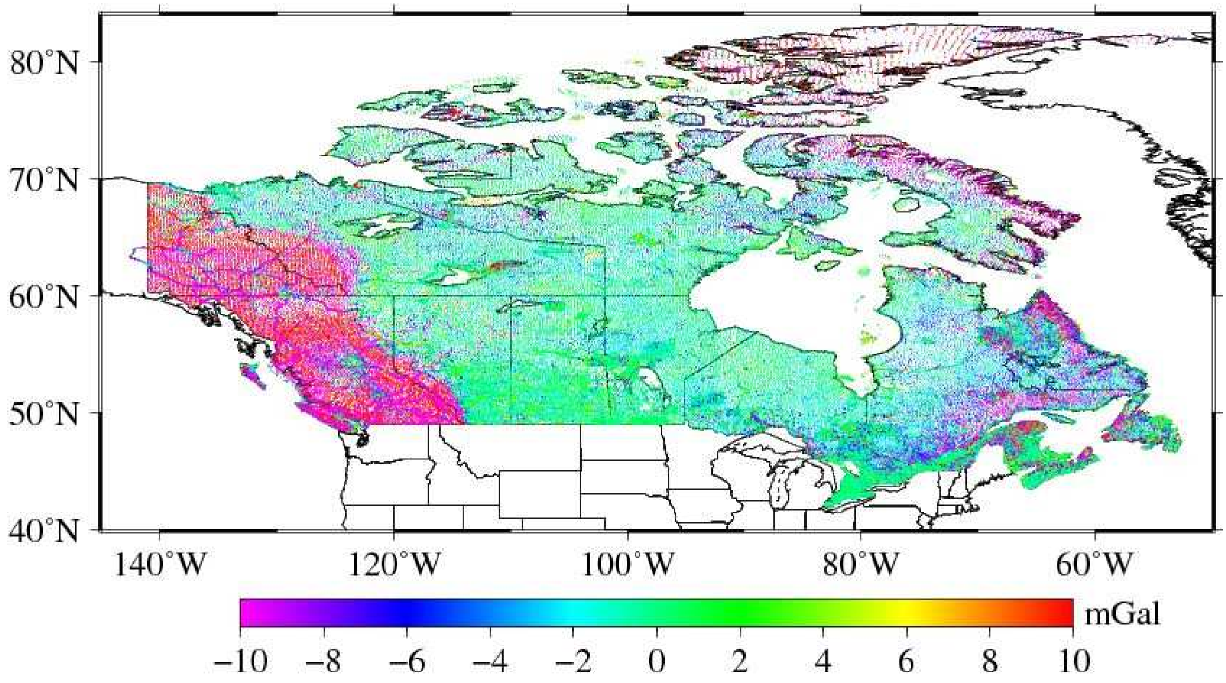

Figure 5.5 Differences between the free-air gravity anomalies and the gravity anomalies synthesized from EGM2008 at 231,079 land points.

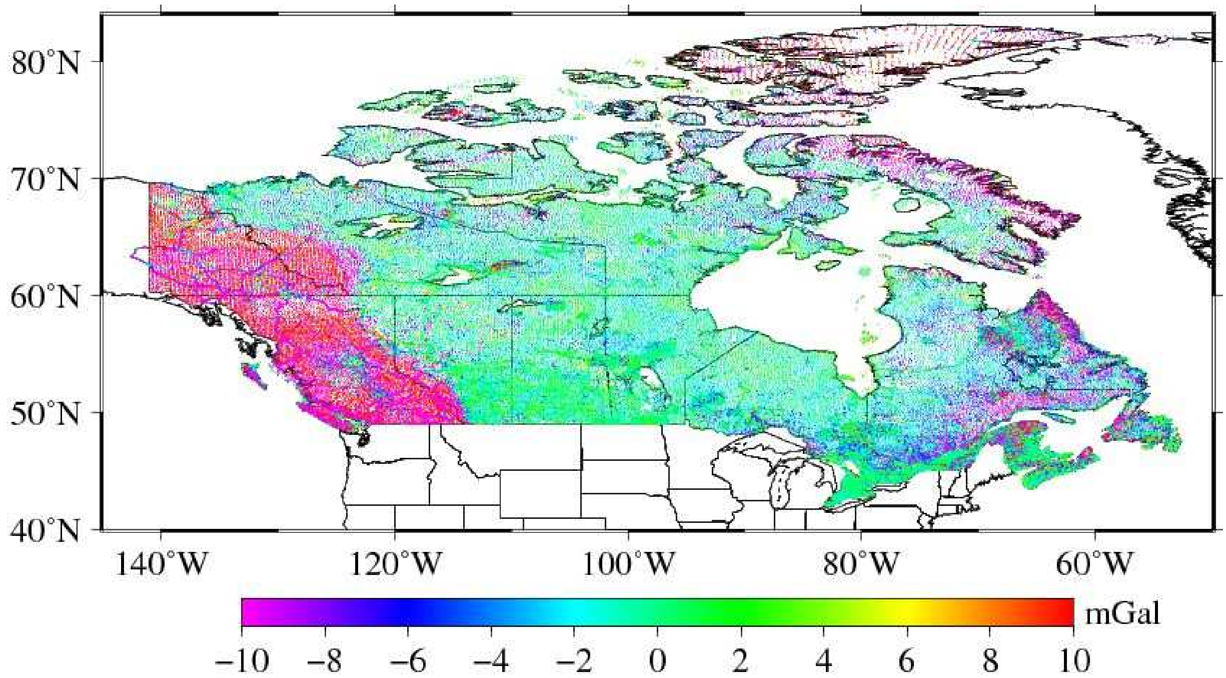

Figure 5.6 Differences between the free-air gravity anomalies and the gravity anomalies synthesized from EIGEN-6C4 at 231,079 land points.

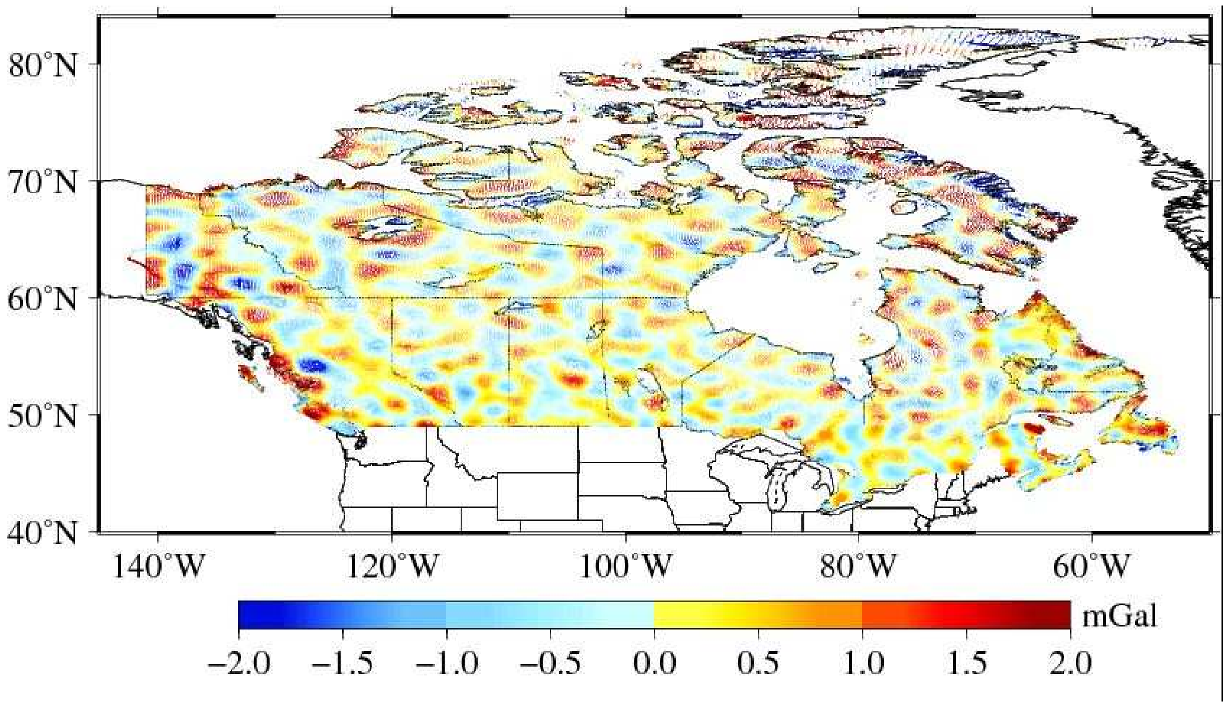

Figure 5.7 Differences between the free-air gravity anomalies synthesized from EIGEN-6C4 and EGM2008 at 231,079 land points.

On the other hand the better performance of EIGEN-6C4 than EGM2008 in the GPS-Levelling validation suggests that the GOCE components in EIGEN-6C4 are slightly better than the corresponding terrestrial components in EGM2008. Figure 5.7 also shows that significant differences generally correlate with relatively sparse and erroneous land gravity data coverage in the western and northern Canada as Figure 4.2 shows.

6 Conclusions

In this study, we analysed seven global geopotential models that are founded on GRACE or/and GOCE observations. The models comprise two recent GRACE-only models (GGM05S and ITSG-Grace2014), two GOCE-only models (TIM-R4 and TIM-R5), two combined GRACE and GOCE models (DIR-R4 and DIR-R5), and one extra high degree model (EIGEN-6C4) that includes the integration of terrestrial and altimetry-derived gravity data. The analysis also includes CGG2013, the geoid model realizing the new vertical datum in Canada, and EGM2008 as baselines. These nine models were validated against three types of datasets in Canada: GPS-Levelling data, astronomic deflections of the vertical and terrestrial land gravity data. We conclude:

1. The GRACE-only models (GGM05S and ITSG-Grace2014) start to deteriorate from spherical harmonic degree 150 in terms of GPS-Levelling validation. However, ITSG-Grace2014 can still perform significantly better than GGM05S up to degree 180 (being the maximum expansion).
2. The GOCE-only models (TIM-R4 and TIM–R5) perform as well as the GRACE-only models below degree 150 in the GPS-Levelling validation. This indicates that the GRACE advantage over GOCE for the lower degrees is not captured by the GPS-Levelling data.
3. The GGMs that include the fifth release of GOCE data (TIM-R5 and DIR-R5) outperform the corresponding R4 models for degrees higher than 180 except in Newfoundland where DIR-R4 outperforms DIR-R5. Most importantly, the R5 models perform steadily beyond degree 200 with an estimated cumulative error smaller than 4-5 cm in terms of GPS-Levelling validation.
4. EGM2008 and EIGEN-6C4 provide similar statistical comparison (13 mGal) in terms of validation against the Canadian terrestrial gravity data over land. The two models directly or indirectly makes use of the Canadian data in their development. The only difference is that EIGEN-6C4 uses less terrestrial gravity data than EGM2008 in the frequency band that includes GOCE measurements. On the other hand, the GOCE contribution in EIGEN-6C4 can be measured against the GPS-Levelling data. EIGEN-6C4 better results than EGM2008 indicates that the GOCE components are more accurate than the corresponding components of the terrestrial gravity data.
5. The regional geoid models based on the R5 models perform slightly better than CGG2013 (L = 180) in the GPS-Levelling validation. It suggests that the R5 models could improve geoid modelling in Canada, allowing a higher degree of modification of the Stokes kernel function (e.g., L = 210). This means a more homogenous solution across Canada and reduction of possible regional systematic errors in the terrestrial gravity data.
6. For the GGMs that include GRACE and GOCE data, we can observe striping patterns indicating possibly that the GRACE data carry too much weight in the models. The striping patterns may be the cause of poorer performance of DIR-R5 than DIR-R4 in Newfoundland.

As for the astronomic deflections, they contain higher frequency components than the regional geoid models causing the omission errors in the comparisons. They compared better with regional geoid models than GGMs such as EGM2008 and EIGEN-6C4 because the former includes relatively higher frequency components. The integration of different GRACE and/or GOCE models in the development of regional geoid models does not influence the statistics of the comparison to astronomic deflections because the GOCE updates are below the error level of the deflections data. It may be feasible to make use of astronomic deflections in evaluating satellite models with a regional geoid model, but they would need to be much more accurate (< 0.1 arcsec).

Acknowledgements: We would like to thank the two anonymous reviewers for their constructive comments and suggestions, and Editor, Dr. Thomas Gruber.

Appendix A: Topographical Term C_{T} for the Geoid Computation from a Global Geopotential Model (GGM)

The geoid can be computed according to Bruns's theorem (Heiskanen and Moritz 1967):

$$N(\Omega) = \frac{T^*(\Omega)}{\gamma_{\mathrm{E}}} \qquad (A1)$$

$T^*(\Omega)$ is the disturbing potential on the geoid inside the topography, and γ_{E} is normal gravity on the geoid.

The disturbing potential $T^*(\Omega)$ on the geoid cannot be computed directly by the spherical harmonic synthesis from a GGM because of the existence of topographical mass above the geoid, which does not meet the harmonic condition. To deal with the topography, we have developed a parallel approach to the Stokes-Helmert scheme which uses terrestrial gravity data for the determination of the disturbing potential on the geoid (Vaníček and Martinec 1994). It conceptually consists of two steps. First the disturbing potential $T_{\mathrm{GGM}}(r,\Omega)$ from the GGM is transformed into the Helmert disturbing potential $T_{\mathrm{HGGM}}(r,\Omega)$ above and on the Earth's surface (Eq. 8, Huang and Véronneau 2013) as follows:

$$T_{\mathrm{HGGM}}(r,\Omega) = T_{\mathrm{GGM}}(r,\Omega) - \delta V_{\mathrm{DTE}}(r,\Omega) \qquad (A2)$$

where $\delta V_{\mathrm{DTE}}(r,\Omega)$ is the direct topographical effect on geopotential (Eq. 28, ibid). The Helmert disturbing potential can be directly computed downwards on the geoid as follows:

$$T_{\mathrm{HGGM}}(\Omega) = T_{\mathrm{GGM}}(\Omega) - \delta V_{\mathrm{DTE}}(\Omega) \qquad (A3)$$

where $T_{\mathrm{GGM}}(\Omega)$ alone is the fictional disturbing potential on the geoid inside the topography, and is given in (Eq. 9, ibid). Second the disturbing potential ${T^*}_{\mathrm{GGM}}(\Omega)$ on the geoid is computed by adding the primary indirect topographical effect, which restores the topography from the Helmert layer condensation layer, as degree-0 and degree-1 terms as follows:

$${T^*}_{\mathrm{GGM}}(\Omega) = T_0(\Omega) + T_1(\Omega) + T_{\mathrm{HGGM}}(\Omega) + \delta V_{\mathrm{PITE}}(\Omega) \qquad (A4)$$

$$\delta V_{\mathrm{PITE}}(\Omega) = 2\pi G\rho R^2 \sum_{n=0}^{nx} \frac{1}{2n+1} \sum_{m=-n}^{n} \bar{I}_{nm}\bar{Y}_{nm}(\Omega) \qquad (A5)$$

$$\bar{I}_{nm} = -(n+1)(t^2)_{nm} - \frac{(n+1)(n-2)}{3}(t^3)_{nm} - \frac{(n+1)n(n-1)}{12}(t^4)_{nm} \qquad (A6)$$

Combining Equations (A3) and (A4), we get

$${T^*}_{\mathrm{GGM}}(\Omega) = T_0(\Omega) + T_1(\Omega) + T_{\mathrm{GGM}}(\Omega) - \delta V_{\mathrm{DTE}}(\Omega) + \delta V_{\mathrm{PITE}}(\Omega) \qquad (A7)$$

By Brums's theorem, we get

$$N_{\text{GGM}}(\Omega) = N_0(\Omega) + N_1(\Omega) + N_{\text{GGM}}(\Omega) + C_{\text{T}}(\Omega) \qquad (A8)$$

where the C_{T} is given by

$$C_{\text{T}}(\Omega) = \frac{-\delta V_{\text{DTE}}(\Omega) + \delta V_{\text{PITE}}(\Omega)}{\gamma_{\text{E}}} \qquad (A9)$$

The sum of the DTE and PITE terms is derived as follows:

$$-\delta V_{\text{DTE}}(\Omega) + \delta V_{\text{PITE}}(\Omega) = 2\pi G\rho R^2 \sum_{n=0}^{nx} \sum_{m=-n}^{n} \overline{\Lambda}_{nm} \overline{Y}_{nm}(\Omega) \qquad (A10)$$

For the fourth order of approximation, we have

$$\overline{\Lambda}_{nm} = -(t^2)_{nm} - \frac{2}{3}(t^3)_{nm} - \frac{(n+1)n}{12}(t^4)_{nm} \qquad (A11)$$

where $t = {}^{H}/_{R}$, and

$$\left(t^k\right)_{nm} = \frac{1}{4\pi}\int_{\Omega} t^k \overline{Y}_{nm}(\Omega) d\Omega \qquad (A12)$$

Sjöberg (Eq. 23, 2007) derived an equivalent equation to (A9) to the 3rd order approximation, and called this term as the topographic bias.

It should be pointed that Rapp (1997) first derived equations for this correction by upward continuing the height anomaly from the reference ellipsoid to the Earth's surface followed by a conversion from the height anomaly to the geoid. In Rapp's upward continuation, only the first-order gradient of the height anomaly was used. Hirt (2012a) improved Rapp's approach by considering higher order gradient terms of the height anomaly with radius. One advantage of equation (A9) is that it is expressed in the spherical harmonic form, and can match the spectral content of GGM with the digital topographic models exactly. A comparison of the two approaches is theoretically and practically interesting but out of the scope of this study.

References:

Bruinsma, S. L., C. Förste, O. Abrikosov, J. C. Marty, M. H. Rio, S. Mulet and S. Bonvalot (2013) The new ESA satellite-only gravity field model via the direct approach. Geophys. Res. Lett., 40, 3607–3612, doi:10.1002/grl.50716

Bruinsma, S. L., C. Förste, O. Abrikosov, J.-M. Lemoine, J.-C. Marty, S. Mulet, M.-H. Rio and S. Bonvalot (2014) ESA's satellite-only gravity field model via the direct approach based on all GOCE data. Geophys. Res. Lett., 41, 7508–7514, doi:10.1002/2014GL062045

Brockmann, J. M., N. Zehentner, E. Höck, R. Pail, I. Loth, T. Mayer-Gürr and W.-D. Schuh (2014) EGM_TIM_RL05: An independent geoid with centimeter accuracy purely based on the GOCE mission. Geophys. Res. Lett., 41, doi:10.1002/2014GL061904

Förste, Ch., F. Flechtner, Ch. Dahle, O. Abrikosov, H. Neumayer, Franz Barthelmes, R. König, S.L. Bruinsma, J.C. Marty, J.-M. Lemoine and R. Biancale (2013) EIGEN-6C3 - the newest High Resolution Global Combined Gravity Field Model based on the 4th Release of the GOCE Direct Approach. Potsdam/Toulouse, Sept. 2013

Förste, Ch., S. L. Bruinsma, O. Abrikosov, J.-M. Lemoine, T. Schaller, H.-J. Götze, J. Ebbing, J.C., Marty, F. Flechtner1, G. Balmino and R. Biancale (2014) EIGEN-6C4 The latest combined global gravity field model including GOCE data up to degree and order 2190 of GFZ Potsdam and GRGS Toulouse. 5th GOCE User Workshop, Paris, 25. – 28.11.2014

Godah, W., M. Szelachowska and J. Krynski (2014) Accuracy assessment of GOCE-based geopotential models and their use for modelling the gravimetric quasigeoid – A case study for Poland. Geodesy and Cartography, 63(1), 3-24, doi:10.2478/geocart-2014-0001

Gruber, Th., P. N. A. M. Visser, Ch. Ackermann and M. Hosse (2011) Validation of GOCE gravity field models by means of orbit residuals and geoid comparisons. J. Geod., 85:845-860, doi:10.1007/s00190-011-0486-7

Heiskanen, W. A. and H. Moritz (1967) Physical geodesy. W.H. Freeman, San Francisco

Guimarães, G., A. Matos and D. Blitzkow (2012) An evaluation of recent GOCE geopotential models in Brazil. Journal of Geodetic Science, 2:144–155, doi:10.2478/v10156-011-0033-8

Hirt, C., U. Marti, B. Bürki, and W. E. Featherstone (2010) Assessment of EGM2008 in Europe using accurate astrogeodetic vertical deflections and omission error estimates from SRTM/DTM2006.0 residual terrain model data. J. Geophys. Res., 115, B10404, doi:10.1029/2009JB007057

Hirt, C., Th. Gruber and W. E. Featherstone (2011) Evaluation of the first GOCE static gravity field models using terrestrial gravity, vertical deflections and EGM2008 quasigeoid heights. J. Geod., 85:723–740, doi:10.1007/s00190-011-0482-y

Hirt, C. (2012a) Efficient and accurate high-degree spherical harmonic synthesis of gravity field functionals at the Earth's surface using the gradient approach. J. Geod., 86:729–744, doi:10.1007/s00190-012-0550-y

Hirt, C., M. Kuhn, W. E. Featherstone and F. Göttl (2012b) Topographic/isostatic evaluation of new-generation GOCE gravity field models. J. Geophys. Res., 117, B05407, doi 10.1029/2011JB008878

Huang, J. and M. Véronneau (2009) Evaluation of the GRACE-Based Global Gravity Models in Canada. Newton's Bulletin, n. 4, 66-72

Huang, J. and M. Véronneau (2013) Canadian gravimetric geoid model 2010. J. Geod., 87:771–790, doi:10.1007/s00190-013-0645-0

Huang, J. and M. Véronneau (2014) A Stokesian approach for the comparative analysis of satellite gravity models and terrestrial gravity data. In U. Marti (ed.), Gravity, Geoid and Height Systems, International Association of Geodesy Symposia 141, doi:10.1007/978-3-319-10837-7_13, Springer

Ince E. S., M. G. Sideris, J. Huang and M. Véronneau (2012) Assessment of the GOCE global gravity models in Canada. Geomatica, 66(2):125-140

Ince, E. S., B. Erol and M. G. Sideris (2014) Evaluation of the GOCE-Based Gravity Field Models in Turkey. In U. Marti (ed.), Gravity, Geoid and Height Systems, International Association of Geodesy Symposia 141, doi:10.1007/978-3-319-10837-7_12, Springer

Janák, J. and M. Pitoňák (2011) Comparison and testing of GOCE global gravity models in Central Europe. Journal of Geodetic Science, 1:333–347

Jekeli, C. (1999) An analysis of vertical deflections derived from high-degree spherical harmonic models. J. Geod., 73: 10 – 22

Jekeli, C. (2000) Heights, the Geopotential, and Vertical Dautms. Report No. 459, Geodetic Science and Surveying, Dept. of Civil and Environmental Engineering and Geodetic Science, The Ohio State Univ., Columbus, Ohio

Li, J., X. Zou, X. Xu and W. Shen (2014) Evaluation of Recent GRACE and GOCE Satellite Gravity Models and Combined Models Using GPS/Leveling and Gravity Data in China. In U. Marti (ed.), Gravity, Geoid and Height Systems, International Association of Geodesy Symposia 141, doi 10.1007/978-3-319-10837-7_9, Springer

Moritz, H (1980) Geodetic Reference System 1980. Bull Geod, 62(2): 187-192

Mayer-Gürr, T., N. Zehentner, B. Klinger and A. Kvas (2014) ITSG-Grace2014: a new GRACE gravity field release computed in Graz. - in: GRACE Science Team Meeting (GSTM). Potsdam

Odera, P. A. and Y. Fukuda (2013) Towards an improvement of the geoid model in Japan by GOCE data: A case study of the Shikoku area. Earth Planets Space, 65, 361–366

Pail, R., et al. (2011) First GOCE gravity field models derived by three different approaches. J. Geod., 85, 819–823, doi:10.1007/s00190-011-0467-x

Pavlis, N. K., S. A. Holmes, S. C. Kenyon and J. K. Factor (2012) The development and evaluation of the Earth Gravitational Model 2008 (EGM2008). J. Geophys. Res., 117, B04406, doi:10.1029/2011JB008916

Rapp, R. H. (1997) Use of potential coefficient models for geoid undulation determinations using a spherical harmonic representation of the height anomaly/geoid undulation difference. J. Geod., 71: 282-289

Rexer, M., C. Hirt, R. Pail and S. Claessens (2013) Evaluation of the third- and fourth-generation GOCE Earth gravity field models with Australian terrestrial gravity data in spherical harmonics. J. Geod., 88(4), 319-333, doi:10.1007/s00190-013-0680-x

Sjöberg, L. E. (2007) The topographic bias by analytical continuation in physical geodesy. J. Geod. (2007) 81:345–350, doi:10.1007/s00190-006-0112-2

Šprlák, M., B. R. Pettersen, O. C. D. Omang, D. I. Lysaker, M. Sekowski and P. Dykowski (2014) Comparison of GOCE Global Gravity Field Models to Test Fields in Southern Norway. In U. Marti (ed.), Gravity, Geoid and Height Systems, International Association of Geodesy Symposia 141, doi:10.1007/978-3-319-10837-7_8, Springer

Tocho, C., G. S. Vergos, and M. C. Pacino (2014) Evaluation of GOCE/GRACE Derived Global Geopotential Models over Argentina with Collocated GPS/Levelling Observations. In U. Marti (ed.), Gravity, Geoid and Height Systems, International Association of Geodesy Symposia 141, doi:10.1007/978-3-319-10837-7_10, Springer

Tapley, B. D., F. Flechmer, S. V. Bettadpur and M. M. Watkins (2013) The status and future prospect for GRACE after the frist decade. Eos Trans. Fall Meet. Suppl., abstract G22A-01

Tsoulis, D. and K. Patlakis (2013) A spectral assessment review of current satellite-only and combined Earth gravity models. Rev. Geophys., 51, 186–243, doi:10.1002/rog.20012

Vaníček P. and Z. Matinec (1994) The Stokes–Helmert scheme for the evaluation of a precise geoid. Man Geod, 19:119–128

Vergos, G. S., V. N. Grigoriadis, I. N. Tziavos and C. Kotsakis (2014) Evaluation of GOCE/GRACE Global Geopotential Models over Greece with Collocated GPS/Levelling Observations and Local Gravity Data. In U. Marti (ed.), Gravity, Geoid and Height Systems, International Association of Geodesy Symposia 141, doi:10.1007/978-3-319-10837-7_11, Springer

Voigt, C. and H. Denker (2014) Regional validation and combination of GOCE gravity field models and terrestrial data. In: Flechtner, F., et al. (eds), Observation of the System Earth from Space - CHAMP, GRACE, GOCE and Future Missions, Advanced Technologies in Earth Sciences, 139-145, doi:10.1007/978-3-642-32135-1_18, Springer

Wang, Y. M. (2009) Investigation of the topographic effect by using high degree spherical harmonic expansion. IAG 2009 Scientific Assembly, Buenos Aires, Argentine, August 31-September 4, 2009